



Title	Enhanced cementation of gold via galvanic interactions using activated carbon and zero-valent aluminum: A novel approach to recover gold ions from ammonium thiosulfate medium
Author(s)	Jeon, Sanghee; Tabelin, Carlito Baltazar; Takahashi, Hiroataka et al.
Citation	Hydrometallurgy, 191, 105165 <a href="https://doi.org/10.1016/j.hydromet.2019.105165">https://doi.org/10.1016/j.hydromet.2019.105165</a>
Issue Date	2020-01
Doc URL	<a href="https://hdl.handle.net/2115/83730">https://hdl.handle.net/2115/83730</a>
Rights	© 2020. This manuscript version is made available under the CC-BY-NC-ND 4.0 license <a href="http://creativecommons.org/licenses/by-nc-nd/4.0/">http://creativecommons.org/licenses/by-nc-nd/4.0/</a>
Rights(URL)	<a href="https://creativecommons.org/licenses/by-nc-nd/4.0/">https://creativecommons.org/licenses/by-nc-nd/4.0/</a>
Type	journal article
File Information	2_1 Manuscript-Gold recovery_20190920.pdf



**Enhanced cementation of gold via galvanic interactions using activated carbon and zero-valent aluminum: A novel approach to recover gold ions from ammonium thiosulfate medium**

Sanghee Jeon<sup>a, \*</sup>, Carlito Baltazar Tabelin<sup>b</sup>, Hirotaka Takahashi<sup>c</sup>, Ilhwan Park<sup>a</sup>, Mayumi Ito<sup>a</sup>,  
Naoki Hiroyoshi<sup>a</sup>

<sup>a</sup>Laboratory of Mineral Processing and Resources Recycling, Division of Sustainable Resources Engineering, Faculty of Engineering, Hokkaido University, Kita 13, Nishi 8, Kita-ku, Sapporo 060-8628, Japan

<sup>b</sup>School of Minerals and Energy Resources Engineering, The University of New South Wales, Sydney, NSW 2052, Australia

<sup>c</sup>Laboratory of Mineral Processing and Resources Recycling, Division of Sustainable Resources Engineering, Graduate School of Engineering, Hokkaido University, Kita 13, Nishi 8, Kita-ku, Sapporo 060-8628, Japan

\*Corresponding author. Tel.: +81-11-706-6315

E-mail address: [shjun1121@gmail.com](mailto:shjun1121@gmail.com) (Sanghee Jeon)

Postal address: Division of Sustainable Resources Engineering, Faculty of Engineering, Hokkaido University, Kita 13, Nishi 8, Kita-ku, Sapporo 060-8628, Hokkaido, Japan

## Highlights

- A novel recovery technique for gold ions in ammonium thiosulfate was developed
- Recovery efficiency using single either ZVA1 or activated carbon was negligible
- >99% of gold was recovered employing both of ZVA1 and activated carbon
- Gold was recovered on activated carbon attached to ZVA1

## **Abstract**

In gold (Au) hydrometallurgy, ammonium thiosulfate is the most attractive and promising alternative to conventional lixiviants like cyanide or the halides because it is non-toxic, less corrosive and has high selectivity for Au. However, its industrial-scale application for Au extraction is still severely limited because the recovery of dissolved Au from pregnant solutions remains challenging. The present study proposes a novel, simple and effective technique to address this difficulty using zero-valent aluminum (ZVAL) and activated carbon.

Gold recovery was investigated by mixing 0.15 g of ZVAL and/or activated carbon and 10 ml of a solution containing 1 M  $\text{Na}_2\text{S}_2\text{O}_3$ , 0.5 M  $\text{NH}_3$ , 0.25 M  $(\text{NH}_4)_2\text{SO}_4$  and 10 mM  $\text{CuSO}_4$  with 100 mg/l of dissolved Au in a constant temperature water bath shaker at 25°C for 24 h. Gold recovery from the ammonium thiosulfate solution was negligible when only ZVAL or activated carbon was added. When ZVAL and activated carbon were both present in the ammonium thiosulfate solution, however, over 99% of Au ions were successfully recovered. Scanning electron microscopy with energy dispersive X-ray spectroscopy (SEM-EDX) observations of the solid residues indicate that Au was predominantly deposited on activated carbon attached to ZVAL. Based on the rest potentials of these two materials, their synergistic effect on Au recovery could be attributed to the formation of numerous galvanic cells in solution where ZVAL acted as anodes (i.e., primary electron donor) while activated carbon acted as the cathode onto which Au ions are reduced via cementation to elemental Au.

**Keywords:** Gold recovery, Cementation, Ammonium thiosulfate solution, Activated carbon, Aluminum

## 1. Introduction

Cyanide and/or halide leaching are the most commonly employed hydrometallurgical techniques to extract gold (Au) from both primary and secondary resources (Calderon et al., 2019; Ha et al., 2010; Jeon et al., 2018a; Kim et al., 2018; Langhans et al., 1992). Although effective, cyanide is toxic to human health, difficult to handle and transport, and harmful to the environment while the halides (e.g., aqua regia) are strongly corrosive and unselective (Jeon et al., 2017). Because of these critical drawbacks, several alternative lixivants for Au are being developed and among them, ammonium thiosulfate is the most promising because it is non-toxic, has high selectivity for Au and is less corrosive (Arima et al., 2002; Jeon et al., 2018a; Karavasteva, 2010). Despite these advantages, the industrial application of ammonium thiosulfate is still limited primarily because of two reasons: (1) the recovery of dissolved Au from ammonium thiosulfate pregnant solutions remains difficult, and (2) conventional recovery techniques like adsorption and reductive precipitation (i.e., cementation) are ineffective in ammonium thiosulfate media. Jiexue and Quian (1989), for example, only recovered ~30% of dissolved Au using activated carbon in their thiosulfate system, which they attributed to the low adsorption affinity of the Au-thiosulfate complex ( $\text{Au}(\text{S}_2\text{O}_3)_2^{3-}$ ) to activated carbon. Similarly, Navarro et al. (2006) reported Au recovery of only 13% on activated carbon under the following conditions: 10 mg/l of gold, 0.8 M of  $\text{NH}_4\text{OH}$ , 0.2 M of  $\text{S}_2\text{O}_3^{2-}$ , pH of 10.5, temperature of 25°C, and recovery time of 8 h. Gallagher et al. (1990) compared the adsorption on activated carbon of the Au-thiosulfate complex with several Au-cyanide complexes and found that the adsorption of Au-thiosulfate complex was the least favorable because the affinity of Au-complexes to activated carbon strongly depended on the type of ligand and follows this order:  $\text{SCN}^- > \text{SC}(\text{NH}_2)_2 > \text{CN}^- > \text{S}_2\text{O}_3^-$ .

Aside from adsorption, dissolved Au in ammonium thiosulfate pregnant solutions could be recovered via reductive precipitation or cementation, an electrochemical process whereby

Au ions are reduced and deposited as elemental Au onto the surface of metals like zinc (Zn) and copper (Cu) that acted as electron donors or reductants (Jeon et al., 2018). Unfortunately, this approach suffers from the excessive amount of Zn and Cu needed for Au recovery because these metallic reductants easily dissolve in ammonium thiosulfate solutions (Alymore and Muir, 2001; Arima et al., 2002; Berezowsky and Sefton, 1979; Guerra et al., 1999; Jeon et al., 2018a). Aluminum (Al) could be another good candidate for Au recovery because of its low standard redox potential (Arima et al., 2002). Unfortunately, Al is easily oxidized in moist air, so its surface is rapidly covered with an aluminum oxyhydroxide film that protects the metal from reductively dissolving especially in solutions with pH between 6 and 10 (Karavasteva et al., 2010; Panoa et al., 2018; Seng et al., 2019a; Park et al., 2018; 2019a; Tabelin et al., 2017a; Tatsuhara et al., 2013).

In a previous study of the authors that investigated the ammonium thiosulfate leaching of Au from printed circuit boards (PCBs), it was reported that Au extraction efficiency was low especially at high solid-to-liquid ratios because extracted Au ions were readily re-deposited onto coexisting metals in PCBs during leaching (Jeon et al., 2018b, 2019). This interesting phenomenon of enhanced Au cementation in ammonium thiosulfate solution was attributed by the authors to galvanic interactions of the various metals found in PCBs (e.g., Cu and Al) that made electron transfer to Au-thiosulfate complex easier. Galvanic interaction is a phenomenon that has also been well reported in mineral processing (Rabieh et al., 2018; Seng et al., 2019b), flotation of complex sulfide ores (Majima, 1969; Allison et al., 1972), and acid/neutral mine drainage formation (Chopard et al., 2017; Tabelin et al., 2017b). In other words, Al and Cu formed numerous galvanic cells composed of Al as the anode (i.e., primary electron donor) and Cu as the cathode (i.e., electron acceptor), a configuration that created an electron pathway between Al and Au-thiosulfate complex (Jeon et al., 2018b). Cu-Al galvanic interactions interfered with and limited the extraction of Au from PCBs in ammonium thiosulfate solution

but by looking at these results from another perspective, a promising way to recover Au ions from ammonium thiosulfate solution was discovered. In this study, a novel approach to recover Au ions from ammonium thiosulfate solutions based on galvanic interactions between zero-valent Al (ZVAI) and activated carbon is introduced. Activated carbon was selected instead of Cu due to the following reasons: (1) it does not dissolve in ammonium thiosulfate solution, (2) it could be regenerated, and (3) it is ubiquitous and cheap.

## **2. Materials and methods**

### 2.1 Materials

ZVAI (99.99%, Wako Pure Chemical Industries, Ltd., Japan) and activated carbon (99.99%, Wako pure Chemical Industries, Ltd., Japan) having about 800-1500 m<sup>2</sup>/g of specific surface area were used to recover Au ions from ammonium thiosulfate solutions (Li et al., 2002; Oda and Nakagawa, 2003).

### 2.2 Characterization of the materials

Particle size distributions and zeta potentials of activated carbon and ZVAI were determined by laser diffraction (Microtrac® MT3300SX, Microtrac Inc., Japan) and Zetasizer Nano-series with MPT-2 multi-purpose titration system (Malvern Corporation, UK), respectively. For the zeta potential measurements, the pH of 10 mg of activated carbon or aluminum in 0.01 M potassium chloride solution was adjusted automatically from 2.0 to 12.0 with 0.1 M hydrochloric acid or sodium hydroxide solution at 25°C. Moreover, surface characterization of ZVAI was done by attenuated total reflectance Fourier transform infrared (ATR-FTIR) spectroscopy (FT/IR-6200 HFV and ATR Pro One attachment equipped with a diamond prism, Jasco Analytical Instruments, Japan).

### 2.3 Recovery of gold ions from ammonium thiosulfate solution

The stock ammonium thiosulfate solutions containing ~100 mg/l of Au ions (i.e., Au-ammonium thiosulfate solution) was prepared by dissolving 0.01 g of gold powder (99.999%, Wako Pure Chemical Industries, Ltd., Japan) in 100 ml of ammonium thiosulfate solution containing 1 M of Na<sub>2</sub>S<sub>2</sub>O<sub>3</sub>, 0.5 M of NH<sub>3</sub>, 0.25 M of (NH<sub>4</sub>)<sub>2</sub>SO<sub>4</sub> and 10 mM of CuSO<sub>4</sub> (pH between 9.5 and 10) using a 300-ml Erlenmeyer flask shaken in a thermostat water bath shaker at 25 °C for 24 h with constant shaking amplitude and frequency of 40 mm and 120 min<sup>-1</sup>, respectively.

To evaluate the recovery of dissolved Au from ammonium thiosulfate solution, 0.15 g of ZVAI and/or 0.15 g of activated carbon were mixed with 10 ml of Au-ammonium thiosulfate solution in 50-ml Erlenmeyer flasks at 25 °C (shaking amplitude of 40 mm and frequency of 120 min<sup>-1</sup>). After 24 h, the filtrate and residue were separated by filtration using 0.2 μm syringe-driven membrane filters (LMS Co., Ltd., Japan). The residues were washed thoroughly with deionized water (18 MΩ·cm, Mill-Q<sup>®</sup> Integral Water Purification System, Merck Millipore, USA), dried in a vacuum oven at 40°C and analyzed by scanning electron microscopy with energy dispersive X-ray spectroscopy (SEM-EDX, Superscan SSX-550, Shimadzu Corporation, Japan). Meanwhile, the concentrations of Au ions remaining in the filtrates were analyzed by inductively coupled plasma atomic emission spectroscopy (ICP-AES) (ICPE-9820, Shimadzu Corporation, Japan) (margin of error = ± 2%) and Au recovery ( $Au_R$ ) was calculated according to the following equation:

$$Au_R = \frac{[Au_B] - [Au_A]}{[Au_B]} \quad (1)$$

where  $[Au_B]$  and  $[Au_A]$  denote the concentrations of dissolved Au before and after the recovery experiments, respectively. Note that dissolved Au concentrations before and after the recovery experiments were measured and the recovery experiments were done in triplicates to ascertain that the observed trends are statistically significant.

### 3. Results and discussion

#### 3.1 Characterization of activated carbon and zero-valent aluminum

The particle size distributions of activated carbon and ZVAI used in this study were in the range of 2-228  $\mu\text{m}$ , and 6-80  $\mu\text{m}$ , respectively (Fig. 1(a) and 1(b)). The  $D_{50}$  of the former and latter were about 32 and 20  $\mu\text{m}$ , indicating that the particle size distributions of both samples are quite similar. Zeta potentials of the samples with pH are illustrated in Fig. 2, and the results showed that ZVAI has a positive charge below pH 8 and a negative charge at above pH 8. In contrast, activated carbon has a positive charge at pH below 3 and is negatively charged from 3.5 to 12. These zeta potential results could be a reason why sole activated carbon and aluminum could not recover gold-thiosulfate complex ( $\text{Au}(\text{S}_2\text{O}_3)_2^{3-}$ ) in the range of pH 9-10 solution.

Since aluminum powder used in this study is not only quite fine in size but also have properties that are easily oxidized, the surface is likely to have been oxidized, hence FTIR was used to elucidate the surface of the aluminum powder (Fig. 3). The strong peaks at 770 are assigned to Al=O vibration band in AlOOH, and an absorption band appeared at 1065 is characteristic of Al—O stretching vibration (Ram, 2001). The spectrum has bands at 580, 1400, 1635, and 1690  $\text{cm}^{-1}$  due to the formation of an amorphous  $\text{AlO}(\text{OH}) \cdot n\text{H}_2\text{O}$  structure. This fraction phase is limited in find particles as it consists of only part of their surface in a thin surface layer (Aluminum Oxide, 2016; Alexander et al., 2015; Ram., 2001). Deconvolution of the broad absorption between 2600 to 3600 further identified several important stretching modes of amorphous  $\text{AlO}(\text{OH}) \cdot n\text{H}_2\text{O}$  structure (2670, and 2700  $\text{cm}^{-1}$ ), and Al—O (2940  $\text{cm}^{-1}$ ) (Ram., 2001; Tabelin et al., 2017a). Deconvolution of these peaks showed that it is composed

of three distinct bands at 3092, 3120, and 3270  $\text{cm}^{-1}$ , and those three peaks are assigned to O—H coordinated with aluminum ions (i.e.,  $\text{AlOOH}$ ) (Ram., 2001; Tabelin et al., 2017a). It is interesting to note that the pure ZVAI (i.e., 99.99%) used in the recovery experiments is already oxidized and is covered with a thin oxyhydroxide film.

### 3.2 Recovery of gold ions from ammonium thiosulfate medium

Figure 4 shows the recovery of Au in ammonium thiosulfate solution using activated carbon, ZVAI, and an ZVAI-activated carbon mixture. The results showed that when only activated carbon or ZVAI was added, Au recovery from the solution was negligible. The limited ability of ZVAI to recover Au ions from ammonium thiosulfate medium could be attributed to the oxyhydroxide/oxide film on it that inhibited the cementation of Au ions (Fig. 3) (Jeon et al., 2018b; Seng et al., 2019a; Syed, 2012). Meanwhile, the low affinity of Au-thiosulfate complex to activated carbon could explain why Au recovery by activated carbon was negligible as noted previously by Gallagher et al. (1990) as well as zeta potential results in Fig. 2. Individually, neither of these two materials could recover Au effectively, but when combined, they recovered over 99% of dissolved Au from the ammonium thiosulfate solution, which means that there is a synergistic interaction between ZVAI and activated carbon that promoted Au recovery.

To investigate how this synergistic phenomenon occurred in the ZVAI-activated carbon system, the solid residue was examined by SEM-EDX. Figure 5 shows the backscattered electron (BSE) photomicrograph of ZVAI-activated carbon mixture and the EDX spectra of several representative points (a-1, a-2, and a-3). Point a-1 had Al and O signals, so this region is the surface of ZVAI while Point a-2 corresponded to the surface of activated carbon because of the strong signal of carbon (C). In comparison, Point a-3 located in an area brighter than the background (i.e., ZVAI surface) showed the peaks of Au and Cu together with Al, C, O and sulfur (S). Multiple EDX point analyses of more than 30 points on randomly

selected particles with prominent bright areas in the BSE image showed that Au and C signals were detected together 90% of the time. The rest potential of aluminum in Au-thiosulfate solution is between  $-0.5$  and  $-0.3$  V (vs. SHE) while that of activated carbon is around  $0.34$ – $0.39$  V (vs. SHE) (Tanahashi et al., 1990), suggesting that ZVAl likely acted as the primary electron donor (i.e., anode) and the attached activated carbon served as electron pathway (i.e., cathode) from ZVAl to Au-thiosulfate complex, a configuration that promoted both galvanic interactions and Au cementation. There are two possible mechanisms for the transfer of electrons between ZVAl and activated carbon that promoted galvanic interactions (Fig. 6): (1) via transfer through the Al-oxyhydroxide layer (Fig. 6(a)), and (2) via direct contact along cracks in the Al-oxyhydroxide coating on ZVAl (Fig. 6(b)). The thin Al-oxyhydroxide film on ZVAl is relatively brittle and prone to cracking (Zeng et al., 2013), so a portion of this coating was likely removed via impact or attrition due to the shaking motion of the recovery experiments the facilitated the first mechanism. Meanwhile, the possible transfer of electrons through the Al-oxyhydroxide layer could be explained via the quantum tunneling effect (Ke et al., 2016).

Based on these results, galvanic interactions between two materials (e.g., ZVAl and activated carbon) with different redox/rest potentials could be utilized as a simple and effective way to recover dissolved Au from ammonium thiosulfate medium, which would likely have revolutionary implications on how Au is extracted and recovered not only from natural ores but also from electronic wastes and other secondary sources. Moreover, this new method could be applied to the recovery and/or removal of persistent redox-active hazardous elements like heavy metals (e.g., Cu, nickel (Ni), cadmium (Cd), and lead (Pb)) and toxic metalloids (e.g., arsenic (As) and selenium (Se)) from groundwater (Huyen et al., 2019a, b; Tabelin et al., 2009; 2014; Tamoto et al., 2015), mine drainage (Park et al., 2019b; Tabelin et al., 2009; Tomiyama et al., 2019) and wastewater (Nazari et al., 2017; Tabelin et al., 2018; 2019).

#### **4. Conclusion**

In Au hydrometallurgy, ammonium thiosulfate has been highlighted since 2000 as a promising alternative to cyanide and the halides because it is non-toxic, is only mildly corrosive, and has high selectivity for Au. In spite these advantages over conventional lixiviants, the application of ammonium thiosulfate leaching in commercial hydrometallurgical operations remains limited primarily because of difficulties in the recovery Au ions from ammonium thiosulfate pregnant solutions. In this study, a simple and highly effective Au recovery technique using ZVAI and activated carbon is introduced. The results showed that individually, activated carbon and ZVAI were ineffective to recover dissolved Au from thiosulfate solution. However, the presence of both ZVAI and activated carbon induced synergy via the formation of galvanic cells that promoted cementation and recovered over 99% of dissolved Au from the thiosulfate solution. This novel and simple technique will likely have important implications on Au hydrometallurgy because it is efficient, eco-friendly and safe. Moreover, it could be utilized for the removal and/or recovery of redox-active persistent contaminants in the environment that are difficult to treat using traditional techniques like adsorption and precipitation.

#### **References**

- Al-Abadleh, H.A., Grassian, V.H., 2003. FT-IR study of water adsorption on aluminum oxide surfaces. *Langmuir*, 19, 341–347.
- Alexander, S., Moorow, L., Lord, A.M., Dunnill, C.W., Barron, A.R., 2015. pH-responsive octylamine coupling modification of carboxylated aluminum oxide surfaces. *J. Mater. Chem. A*. 3. 10052–10059.

- Aluminum oxide, 2016. Deposition and Characterization of Aluminum Oxide Thin Films. <http://aluminiumoxidekirikaza.blogspot.com/2016/05/ftir-spectrum-of-aluminium-oxide.html> (Accessed 12 September 2019).
- Arima, H., Fujita, T., Yen, W., 2002. Gold Cementation from Ammonium Thiosulfate Solution by Zinc, Copper and Aluminum Powders. *Mater. Trans.* 43 (3), 485–493.
- Allison, S. A., Goold, L. A., Nicol, M. J., Granville, A., 1972. A determination of the products of reaction between various sulfide minerals and aqueous xanthate solution, and a correlation of the products with electrode rest potentials. *Metallurgical Transactions.* 3, 2613–2618. <https://doi.org/10.1007/BF02644237>
- Alymore, M.G., Muir, D.M., 2001. Thiosulfate leaching of gold—A review. *Miner. Eng.* 14 (2), 135–174.
- Berezowsky, R.M., Sefton, V.B., 1979. Recovery of gold and silver from oxidation leach residues by ammonium thiosulfate leaching. Paper presented at AIME Annual Meeting, New Orleans, L.A., 102–105.
- Calderon, A.R.M., Alorro, R.D., Tadesse, B., Yoo, K., Tabelin, C.B., 2019. Evaluation of Maghemite-Rich Iron Oxide Composite Prepared from Magnetite as Adsorbent for Gold from Chloride Solution. *JOM*, 1–8.
- Chopard, A., Plante, B., Benzaazoua, M., Bouzahzah, H., Marion, P., 2017. Geochemical investigation of the galvanic effects during oxidation of pyrite and base-metals sulphides. *Chemosphere* 166, 281–291.
- Corti, C., Holiday, R., 2009. *Gold: Science and Applications*, first ed. CRC Press, London, New York, 240.
- Diggle, J.W., Downie, T.C., Goulding, C.W., 1969. Anodic oxide films on aluminum. *Chem. Rev.* 69 (3), 365–405.

- Gallagher, N.P., Hendrix, J.L., Milosavljevic, E.G., Nelson, J.H., Solujic, L., 1990. Affinity of activated carbon towards some gold (I) complexes. *Hydrometallurgy* 25, 305–316.
- Guerra, E., Dreisinger, D.B., 1999. A study of the factors affecting copper cementation of gold from ammonium thiosulfate solution. *Hydrometallurgy* 51 (2), 155–172.
- Ha, V.H., Lee, J., Jeon, J., Hai, H.T., Jha, M.K., 2010. Thiosulfate leaching of gold from waste mobile phone. *J. Hazard. Mater.* 178 (1-3), 1115–1119.
- Hiskey, J.B., Lee, J., 2003. Kinetics of gold cementation on copper in ammonium thiosulfate solutions. *Hydrometallurgy* 69 (1-3), 45–56.
- Hsu, Y.J., Tran, T., 1996. Selective removal of gold from copper-gold cyanide liquors by cementation using zinc. *Miner. Eng.* 9 (1), 1–13.
- Huyen, D.T., Tabelin, C.B., Thuan, H.M., Dang, D.H., Truong, P.T., Vongphuthone, B., Kobayashi, M. and Igarashi, T., 2019a. The solid-phase partitioning of arsenic in unconsolidated sediments of the Mekong Delta, Vietnam and its modes of release under various conditions. *Chemosphere* 233, 512–523.  
<https://doi.org/10.1016/j.chemosphere.2019.05.235>
- Huyen, D.T., Tabelin, C.B., Thuan, H.M., Danga, D.H., Truong, P.T., Vongphuthone, B. and Kobayashi, M., 2019b. Geological and geochemical characterizations of sediments in six borehole cores from the arsenic-contaminated aquifer of the Mekong Delta, Vietnam. *Data in Brief*, 104230. <https://doi.org/10.1016/j.dib.2019.104230>
- Jeon, S., Yoo, K., Alorro, R.D., 2017. Separation of Sn, Bi, Cu from Pb-free solder paste by ammonia leaching followed by hydrochloric acid leaching. *Hydrometallurgy* 169, 26–30.
- Jeon, S., Tabelin, C.B., Takahashi, H., Park, I., Ito, M., Hiroyoshi, N., 2018a. Interferences of coexisting copper and aluminum on the ammonium thiosulfate leaching of gold from printed circuit boards of waste mobile phones. *Waste Manage.* 81, 148–156.

- Jeon, S., Ito, M., Tabelin, C.B., Pongsumrankul, R., Kitajima, N., Park, I., Hiroyoshi, N., 2018b. Gold recovery from shredder light fraction of E-waste recycling plant by flotation-ammonium thiosulfate leaching. *Waste Manage.* 77, 195–202.
- Jeon, S., Ito, M., Tabelin, C.B., Pongsumrankul, R., Tanaka, S., Kitajima, N., Saito, A., Park, I. and Hiroyoshi, N., 2019. A physical separation scheme to improve ammonium thiosulfate leaching of gold by separation of base metals in crushed mobile phones. *Minerals Engineering*, 138, pp.168–177.
- Jiexue, H. and Qian, G., Substitute sulfate for sulfite during extraction of gold, *Randol Gold Forum*, Randol International, Colorado, USA, 1991, pp126–132.
- Karavasteva, M., 2010. Kinetics and deposit morphology of gold cemented on magnesium, aluminum, zinc, iron and copper from ammonium thiosulfate-ammonia solutions. *Hydrometallurgy* 104 (1), 119–122.
- Ke, B., Li, Y., Chen, J., Zhao, C. and Chen, Y., 2016. DFT study on the galvanic interaction between pyrite (100) and galena (100) surfaces. *Applied Surface Science*, 367, 270–276.
- Kim, B., Chae, S., Kim, J., Yoo, K., 2018. Oversea Production Status of Gold, Silver, Platinum, and Palladium from Scrap. *J. of Korean Ins. of Resources Recycling* 27(6), 76–83.
- Langhans, J.W., Lei, K.P.V., Carnahan, T.G., 1992. Copper-catalyzed thiosulfate leaching of low-grade gold ores. *Hydrometallurgy* 29 (1-3), 191–203.
- Li, F., Yuasa, A., Ebie, K., Azuma, Y., Hagishita, T., Matsui, Y., 2002. Factors affecting the adsorption capacity of dissolved organic matter onto activated carbon: modified isotherm analysis. *Water Research* 36(18), 4592–4604.
- Liu, C., Shih, K., Gau, Y., Li, F., Wei, L., 2012. Dechlorinating transformation of propachlor through nucleophilic substitution by dithionite on the surface of alumina. *J. Soils Sediments* 12. 724–733.

- Majima, H., 1969. How oxidation affects selective flotation of complex sulphide ores. *Canadian Metallurgical Quarterly*, 8(3), 269-273.
- McDougall, G.J., Hancock, R.D., Nicol, M.J., Wellington, O.L., Copperthwaite, R.G., 1980. The mechanism of the adsorption of gold cyanide on activated carbon. *J. S. Afr. Inst. Min. Metall.* 80 (9), 344–356.
- Miller, J.D., Wan, R.Y., Parga, J.R., 1990. Characterization and electrochemical analysis of gold cementation from alkaline cyanide solution by suspended zinc particles. *Hydrometallurgy* 24 (3), 373–392.
- Navarro, P., Vargas, C., Alonso, M., Alguacil, F.J., 2006. The adsorption of gold on activated carbon from thiosulfate-ammonium solutions. *Gold Bulletin* 39(3), 93–97.
- Nazari, A.M., Radzinski, R. and Ghahreman, A., 2017. Review of arsenic metallurgy: Treatment of arsenical minerals and the immobilization of arsenic. *Hydrometallurgy*, 174, 258–281.
- Nguyen, H.H., Tran, T., Wong, P.L.M., 1997. A kinetic study of the cementation of gold from cyanide solutions onto copper. *Hydrometallurgy* 46 (1-2), 55–69.
- Oda, H., Nakagawa, Y., 2003. Removal of ionic substances from dilute solution using activated carbon electrodes. *Carbon* 41(5), 1037–1047.
- Panao, A.S., Carvalho, J.R., Correia, N.D.S., 2007. Copper removal from sulphuric leaching solutions by cementation. *Semantic Scholar*. 1-12.
- Park, I., Tabelin, C.B., Seno, K., Jeon, S., Ito, M., Hiroyoshi, N., 2018. Simultaneous suppression of acid mine drainage formation and arsenic release by Carrier-microencapsulation using aluminum-catecholate complexes. *Chemosphere*. 205, 414–425. <https://doi.org/10.1016/j.chemosphere.2018.04.088>.
- Park, I., Tabelin, C.B., Seno, K., Jeon, S., Inano, H., Ito, M., Hiroyoshi, N., 2019a. Carrier-microencapsulation of arsenopyrite using Al-catecholate complex: Nature of oxidation

- products, effects on anodic and cathodic reactions, and coating stability under simulated weathering conditions. *Heliyon*, Under review.
- Park, I., Tabelin, C.B., Jeon, S., Li, X., Seno, K., Ito, M. and Hiroyoshi, N., 2019b. A review of recent strategies for acid mine drainage prevention and mine tailings recycling. *Chemosphere* 219, 588–606.
- Poinern, G.E.J., Ali, N., Fawcett, D., 2011. Progress in Nano-Engineered Anodic Aluminum Oxide Membrane Development. *Mater.* 4 (3), 487–526.
- Rabieh, A., Eksteen, J.J., Albijanic, B., 2018. Galvanic interaction of grinding media with arsenopyrite and pyrite and its effect on gold cyanide leaching. *Miner. Eng.* 116, 46–55. <https://doi.org/10.1016/j.mineng.2017.10.018>.
- Ram, S. 2001. Infrared spectral study of molecular vibrations in amorphous, nanocrystalline and  $\text{AlO}(\text{OH}) \cdot n\text{H}_2\text{O}$  bulk crystals. *Infrared Physics & Technology* 42, 547–560.
- Seng, S., Tabelin, C.B., Kojima, M., Hiroyoshi, N., Ito, M., 2019a. Galvanic microencapsulation (GME) using zero-valent aluminum and zero-valent iron to suppress pyrite oxidation. *Mater. Trans.*, 60(2), 277–286.
- Seng, S., Tabelin, C.B., Makino, Y., Chea, M., Phengsaart, T., Park, I., Hiroyoshi, N. and Ito, M., 2019b. Improvement of flotation and suppression of pyrite oxidation using phosphate-enhanced galvanic microencapsulation (GME) in a ball mill with steel ball media. *Minerals Engineering* 143, 105931.
- Syed, S., 2012. Recovery of gold from secondary sources—A review. *Hydrometallurgy* (115-116), 30–51.
- Tabelin, C.B., Igarashi, T., 2009. Mechanisms of arsenic and lead release from hydrothermally altered rock. *J. Hazard. Mater.* 169, 980–990.

- Tabelin, C.B., Igarashi, T., Tamoto, S., Takahashi, R., 2012. The roles of pyrite and calcite in the mobilization of arsenic and lead from hydrothermally altered rocks excavated in Hokkaido, Japan. *J. Geochem. Explor.* 119–120, 17–31.
- Tabelin, C.B., Hashimoto, A., Igarashi, T. and Yoneda, T., 2014. Leaching of boron, arsenic and selenium from sedimentary rocks: II. pH dependence, speciation and mechanisms of release. *Science of The Total Environment* 473, 244-253.
- Tabelin, C.B., Veerawattananun, S., Ito, M., Hiroyoshi, N., Igarashi, T., 2017a. Pyrite oxidation in the presence of hematite and alumina: I. Batch leaching experiments and kinetic modeling calculations. *Sci. Total Environ.* 580, 687–689.
- Tabelin, C.B., Veerawattananun, S., Ito, M., Hiroyoshi, N., Igarashi, T., 2017b. Pyrite oxidation in the presence of hematite and alumina: II. Effects on the cathodic and anodic half-cell reactions. *Sci. Total Environ.* 581–582, 126–135.
- Tabelin, C.B., Igarashi, T., Villacorte-Tabelin, M., Park, I., Opiso, E.M., Ito, M. and Hiroyoshi, N., 2018. Arsenic, selenium, boron, lead, cadmium, copper, and zinc in naturally contaminated rocks: A review of their sources, modes of enrichment, mechanisms of release, and mitigation strategies. *Science of the Total Environment* 645, 1522–1553.
- Tabelin, C.B., Corpuz, R.D., Igarashi, T., Villacorte-Tabelin, M., Ito, M. and Hiroyoshi, N., 2019. Hematite-catalysed scorodite formation as a novel arsenic immobilisation strategy under ambient conditions. *Chemosphere* 233, 946–953.
- Tanahashi, I., Yoshida, A., Nishino, A., 1990. Electrochemical characterization of activated carbon-fiber cloth polarizable electrodes for electric double-layer capacitors. *J. Electrochem. Soc.* 137(10), 3052–3057.
- Tamoto, S., Tabelin, C.B., Igarashi, T., Ito, M. and Hiroyoshi, N., 2015. Short and long term release mechanisms of arsenic, selenium and boron from a tunnel-excavated sedimentary rock under in situ conditions. *Journal of Contaminant Hydrology* 175, 60-71.

- Tatsuhara, T., Arima, T., Igarashi, T. and Tabelin, C.B., 2012. Combined neutralization–adsorption system for the disposal of hydrothermally altered excavated rock producing acidic leachate with hazardous elements. *Engineering geology*, 139, pp.76–84.
- Tomiyama, S., Igarashi, T., Tabelin, C.B., Tangviroon, P. and Ii, H., 2019. Acid mine drainage sources and hydrogeochemistry at the Yatani mine, Yamagata, Japan: A geochemical and isotopic study. *Journal of contaminant hydrology*, 225, 103–502.
- Vilchis-carbajal, S., Gonzalez, I., Lapidus, G.T., 2000. An electrochemical study of gold cementation with zinc powder at low cyanide concentration in alkaline solutions. *J. Appl. Electrochem.* 30, 217–229.
- Wang, Z., Chen, D., Chen, L., 2007. Application of fluoride to enhance aluminum cementation of gold from acidic thiocyanate solution. *Hydrometallurgy* 89 (3-4), 196–206.
- Zeng, J., Li, D., He, Haun, Zhiliu, H., Cuiyun, H., Jialin, Y., 2013. Relationship between aluminum oxide inclusion and porosity in aluminum melt. The 8<sup>th</sup> pacific rim international congress on advanced materials and processing. The Minerals, Metals, & Materials Society (TMS).

### **Figure captions**

**Fig. 1.** Particle size distribution of activated carbon and zero-valent aluminum (ZVAI).

**Fig. 2.** Zeta potential distributions of activated carbon and zero-valent aluminum (ZVAI) with pH.

**Fig. 3.** ATR-FTIR spectrum of zero-valent aluminum (ZVAI).

**Fig. 4** Gold recovery in ammonium thiosulfate solution after 24 h with zero-valent aluminum (ZVAI), activated carbon and a ZVAI-activated carbon mixture.

**Fig. 5.** (a) Back-scattered electron (BSE) photomicrograph of the residue from the ZVAI-activated carbon system, and the corresponding EDX spectra of point (a-1), point (a-2) and point (a-3).

**Fig. 6.** Schematic diagram of possible electron transfer mechanism between ZVAI and activated carbon in ammonium thiosulfate solution: (a) electron transfer through the Al-oxyhydroxide layer and (b) direct contact via cracks within the Al-oxyhydroxide layer.

# Figures

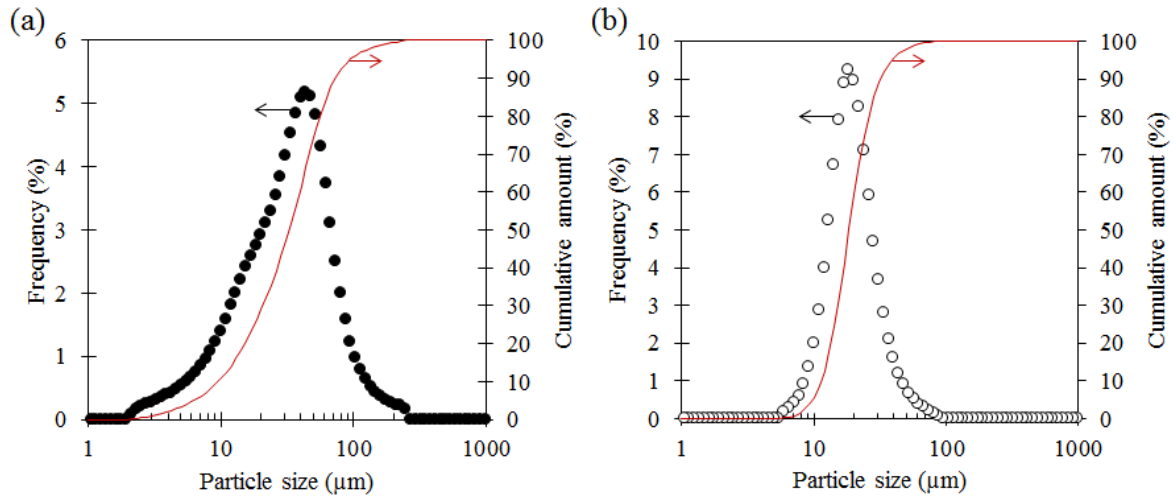


Fig. 1. Particle size distribution of (a) activated carbon and (b) zero-valent aluminum (ZVAI).

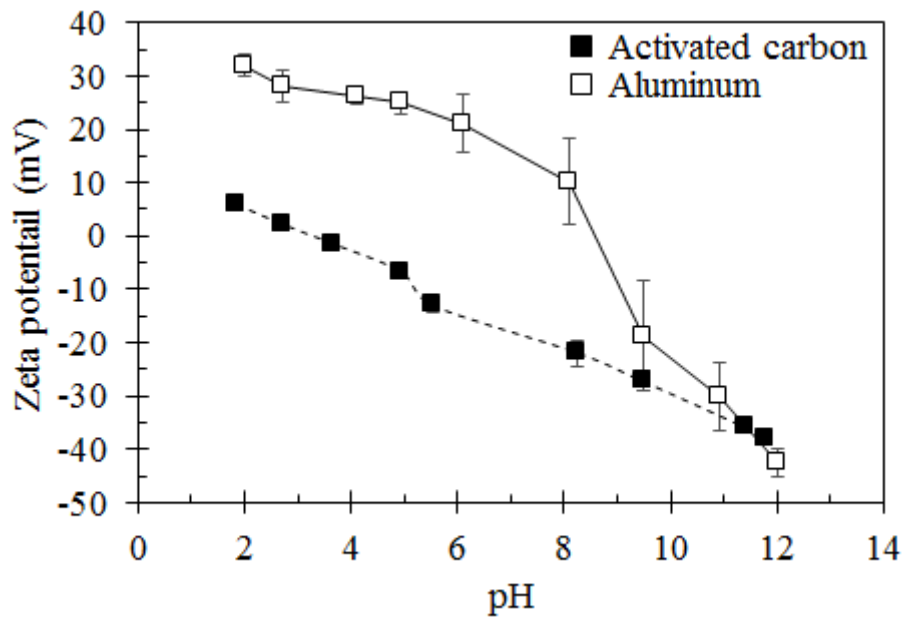
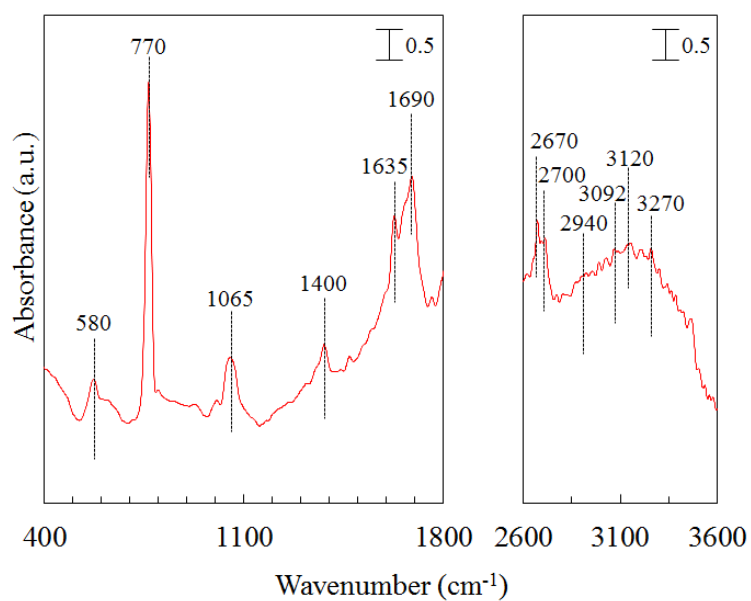
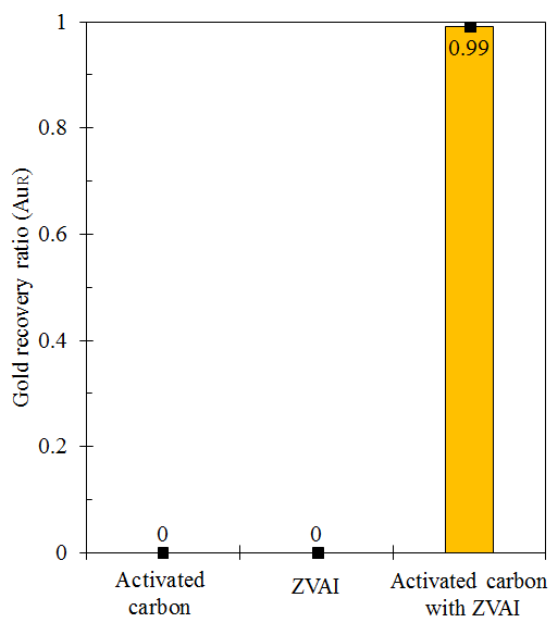


Fig. 2. Zeta potential distributions of activated carbon and zero-valent aluminum (ZVAI) with pH



**Fig. 3.** ATR-FTIR spectrum of zero-valent aluminum (ZVAI)



**Fig. 4.** Gold recovery in ammonium thiosulfate solution after 24 h with zero-valent aluminum (ZVAI), activated carbon and a ZVAI-activated carbon mixture.

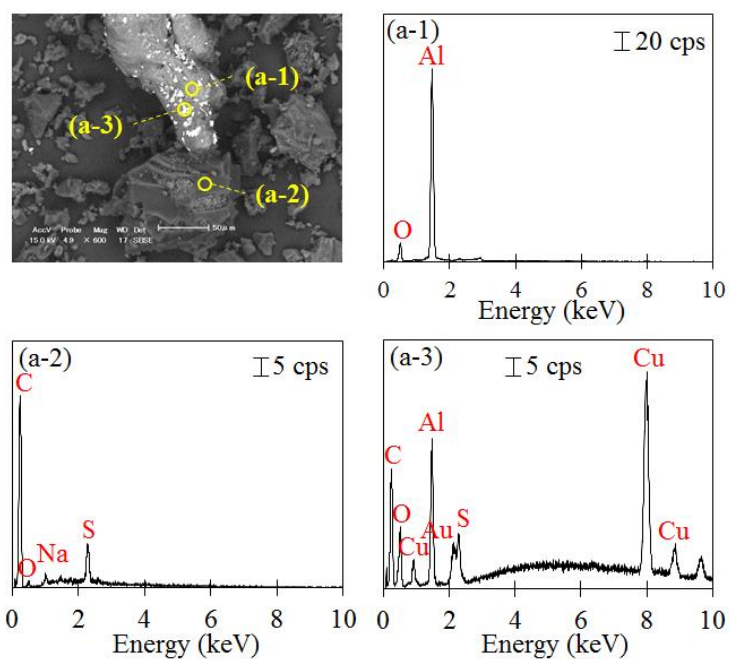


**Fig. 5.** (a) Back-scattered electron (BSE) photomicrograph of the residue from the ZVAI-activated carbon system, and the corresponding EDX spectra of point (a-1), (a-2), and (a-3).

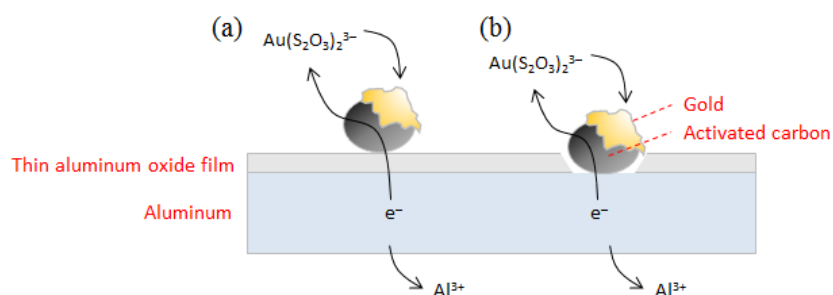


**Fig. 6.** Schematic diagram of possible electron transfer mechanism between ZVAI and activated carbon in ammonium thiosulfate solution: (a) electron transfer through the Al-oxyhydroxide layer and (b) direct contact via cracks within the Al-oxyhydroxide layer.